Contribution from the Department of Chemistry,
The University of North Carolina at Chapel Hill, Chapel Hill, North Carolina 27514

Study of Intradimer and Interdimer Exchange Interactions in $[Cu_2(dien)_2Cl_2](ClO_4)_2$ by Electron Paramagnetic Resonance and Magnetic Susceptibility Measurements

S. K. HOFFMANN,[1] DEBRA K. TOWLE,[2] WILLIAM E. HATFIELD,*[2] PHALGUNI CHAUDHURI,[3] and KARL WIEGHARDT[3]

Received May 15, 1984

EPR spectra of single crystals of the compound $[Cu_2(dien)_2Cl_2](ClO_4)_2$ exhibit a strong merging effect between lines from magnetically nonequivalent dimers in the unit cell. Neither fine structure nor hyperfine structure was resolved down to 77 K. The interdimer exchange integral has been determined to be 0.0030 (1) cm^{-1} at room temperature from a computer simulation of the merging effects. Molecular g factors of individual copper(II) ions were determined from angular-dependence measurements on single crystals in a coplanar three-axial reference system to be $g_z = 2.214$ (3), $g_y = 2.057$ (3), and $g_x = 2.046$ (3). The x, y, and z axes do not coincide closely with the Cu–ligand directions. The line widths of the EPR lines are strongly temperature dependent and increase linearly with temperature from 77 to 250 K. This unusual behavior is explained in terms of an unresolved zero-field splitting resulting from intradimer dipolar coupling. The interdimer exchange integral J' increases with decreasing temperature from 0.0025 cm^{-1} at 380 K to 0.01 cm^{-1} at 77 K as a result of thermal lattice contraction.

Introduction

Studies of magnetic properties of bis(μ-chloro) bimetallic copper(II) complexes[4–6] have shown that the copper ions in most of the bimetallic complexes are antiferromagnetically exchange coupled with small singlet–triplet (ΔE_{ST}) splittings, although examples of triplet ground state, ferromagnetically coupled systems are known.[5] The fine structure in the EPR spectra of complexes with small ΔE_{ST} is generally not resolved either at room temperature or at liquid-nitrogen temperature because of dipolar and exchange interactions in the magnetically condensed systems. In these cases, the high-temperature EPR spectra are determined by the electronic structures of single copper(II) ions and by the interdimer exchange coupling, which averages the EPR line positions of differently oriented dimers in the crystals. In addition, the EPR line widths are very sensitive to dynamical properties of the crystal lattice.

The synthesis, crystal structure, and preliminary magnetic susceptibility and EPR data for $[Cu_2(dien)_2Cl_2](ClO_4)_2$ (dien = diethylenetriamine) have been reported.[7] The compound crystallizes in the space group $Pbn2_1$ with unit cell parameters a = 7.637 (1) Å, b = 13.549 (3) Å, and c = 20.866 (4) Å and with 4 molecules in the unit cell. The compound contains bis(μ-chloro)-bridged dimers with Cu–Cl bridging distances of 2.770 (5), 2.735 (5), 2.313 (5), and 2.266 (5) Å and Cu–Cl–Cu bridging angles of 92.0 and 92.1°. Here, we describe the results of EPR and magnetic susceptibility studies on $[Cu_2(dien)_2Cl_2](ClO_4)_2$, which permit a description of intradimer and interdimer exchange interactions.

Experimental Section

Electron Paramagnetic Resonance. Single crystals suitable for EPR measurements were obtained by very slow (3 weeks) crystal growth from water solution. The crystals were rhombohedral in shape, with the (001) plane being most prominantly developed. EPR spectra were recorded at X-band on a Varian E-109 spectrometer with a rectangular TE_{102} cavity. The magnetic field was calibrated with a DPPH marker, and the frequency was monitored with a Hewlett-Packard 5245L frequency counter. The angular dependence of the spectra was recorded in two reference systems, those being the crystallographic axes system a, b, c, and a coplanar system *1*, *2*, a with axis *1* in the ab plane at an angle of 60° from the a axis. The temperature dependence of the spectra along the a, b, c axes and along the molecular z axis of an individual complex was measured in the temperature range 77–380 K by using an E-4557 Varian variable-temperature accessory. Because of relatively low resolution (splitting/line width ratio) of the EPR spectra, parameters of individual lines were determined for most crystal orientations by computer simulation with a program written for a Tektronix 4052 graphics computer.

Magnetic Susceptibility. Magnetic susceptibility data were collected in the temperature range 2–60 K on a powdered sample by using a PAR Model 155 vibrating-sample magnetometer that was operated at 10 kG. The magnetometer was calibrated with $HgCo(NCS)_4$.[8,9] A calibrated GaAs diode was used to monitor the sample temperature. The data were corrected for diamagnetism of constituent atoms and for temperature-independent paramagnetism of the copper(II) ion (60×10^{-6} cgsu).

Results and Discussion

Magnetic Properties. The molar magnetic susceptibility of a powdered sample is plotted as a function of temperature in Figure 1. The excellent fitting of the inverse susceptibility to a straight line in the temperature range 2–60 K indicates a very small singlet–triplet splitting. Thus, an application of the magnetic susceptibility expression for a pair of exchange-coupled $S = {}^1/_2$ ions is inappropriate since the singlet–triplet splitting is smaller than the Zeeman energy $g\mu_B B$, which is about 1.2 cm^{-1} at B = 10 kG. The more general magnetization expression for a pair of $S = {}^1/_2$ ions was used:

$$M = \frac{Ng\mu_B \sinh (g\mu_B B/kT)}{1 + \exp(-2J/kT) + 2\cosh (g\mu_B B/kT)} \quad (1)$$

Equation 1 was fit to the experimental magnetization data by using a Simplex fitting routine,[10] with g = 2.104 as a constant parameter. This g value is equal to the average value of the **g** tensor principal components determined from EPR spectra. The best fit was found with $2J = +0.4$ (3) cm^{-1} and is represented by the solid lines in Figure 1. The intradimer exchange Hamiltonian is of the form $\mathcal{H} = -2JS_1 \cdot S_2$. The relative accuracy of the singlet–triplet splitting is not very high, but the magnetic data clearly indicate a weak ferromagnetic intradimer coupling. A more accurate singlet–triplet value could be obtained by collecting data below 2 K.

A strong correlation has been found between the singlet–triplet splitting and the quotient ϕ/R in symmetrical bis(μ-chloro)copper(II) bimetallic complexes where ϕ equals the Cu–Cl–Cu bridging angle and R is the longer Cu–Cl distance.[5,6,11] The dimeric unit in $[Cu_2(dien)_2Cl_2](ClO_4)_2$ is not symmetrical, so a value of $\phi/R = 33.5°/Å$ was calculated by averaging bond dis-

(1) Permanent address: Institute of Molecular Physics, Polish Academy of Sciences, 60-179 Poznan, Poland.
(2) The University of North Carolina at Chapel Hill.
(3) Ruhr-Universität, Bochum, West Germany.
(4) Roundhill, S. G. N.; Roundhill, D. M.; Bloomquist, D. R.; Landee, C.; Willett, R. D.; Dooley, D. M.; Gray, H. B. *Inorg. Chem.* **1979**, *18*, 831.
(5) Marsh, W. E.; Patel, K. C.; Hatfield, W. E.; Hodgson, D. J. *Inorg. Chem.* **1983**, *22*, 511.
(6) Marsh, W. E. Ph.D. Dissertation, The University of North Carolina at Chapel Hill, 1982.
(7) Hoffmann, S. K.; Towle, D. K.; Hatfield, W. E.; Wieghardt, K.; Chaudhuri, P.; Weiss, J. *Mol. Cryst. Liq. Cryst.* **1984**, *107*, 161.
(8) Brown, D. B.; Crawford, V. H.; Hall, J. W.; Hatfield, W. E. *J. Phys. Chem.* **1977**, *81*, 1303.
(9) Figgis, B. N.; Nyholm, R. S. *J. Chem. Soc.* **1958**, 4190.
(10) Hatfield, W. E.; Weller, R. R.; Hall, J. W. *Inorg. Chem.* **1980**, *19*, 3285.
(11) Hatfield, W. E. *Comments Inorg. Chem.* **1981**, *1*, 105.

0020-1669/85/1324-1307$01.50/0

Table I. Structural and Magnetic Properties of Bis(μ-chloro)-Bridged Copper(II) Dimers[a]

	compd	R_i(Cu–Cl), Å	R_o(Cu–Cl), Å	Cu–Cl–Cu', deg	ϕ/R_o, deg/Å	$2J$, cm^{-1}	ref
1	$[Cu(dmg)Cl_2]_2$	2.245	2.70	88.0	32.6	+6.3	53–55
2	$[Cu(Me_3en)Cl_2]_2$	2.31	2.74	86.1	31.4	−2.1	56, 57
3	$[Cu(4\text{-Meox})_2Cl_2]_2$	2.38	2.60	84.5	34.4	−2.6	6
4	$[Cu(Guan)Cl_3]_2 \cdot 2H_2O$	2.29	2.45	98.0	40.0	−82.6	58, 59
5	$[Cu(Et_3en)Cl_2]_2$	2.28	2.73	94.8	34.8	+0.1	5
6	$[Cu(4\text{-Metz})(DMF)Cl_2]_2$	2.30	2.72	95.3	35.0	−3.4	64
7	$[Co(en)_3]_2[Cu_2Cl_8]Cl_2$	2.33	2.70	95.2	35.2	−14.6	60, 61
8	$[Cu(TMSO)Cl_2]_2$	2.28	3.02	88.5	29.3	−17.0	62
9	$[Cu(tmen)Cl_2]_2$	2.26	3.15	96.8	30.7	−5.6	57, 63
10	$[Cu(2\text{-pic})_2Cl_2]_2$	2.29	3.36	100.6	29.9	−7.4	64–66
11	$[Cu(dien)Cl]_2(ClO_4)_2$	2.29	2.75	92.0	33.5	+0.4	this work

[a] Abbreviations: dmg = dimethylglyoxime; Me_3en = *N,N,N'*-trimethylethylenediamine; 4-Meox = 4-methyloxazole; Quan = guaninium; Et_3en = *N,N,N'*-triethylethylenediamine; 4-Metz = 4-methylthiazole; en = ethylenediamine; TMSO = tetramethylene sulfoxide; tmen = *N,N,N',N'*-tetramethylethylenediamine; 2-pic = 2-methylpyridine; dien = diethylenetriamine.

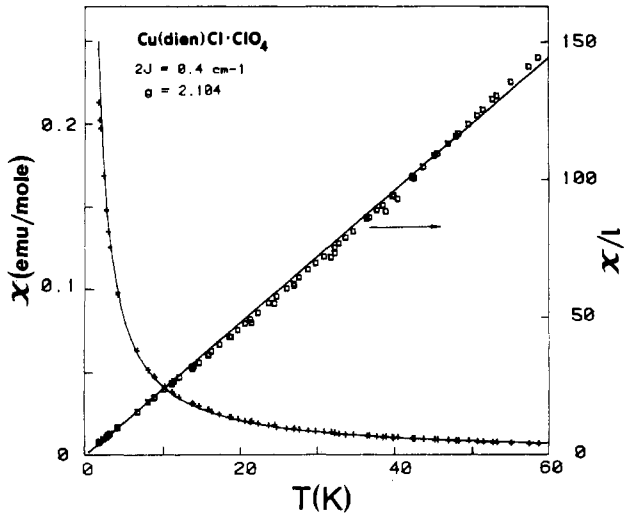

Figure 1. Temperature dependence of the molar magnetic susceptibility χ_m and the inverse susceptibility of $[Cu_2(dien)_2Cl_2](ClO_4)_2$. The solid lines represent the best fit to the magnetization equation (1) with $2J$ = +0.4 cm^{-1} and g = 2.104.

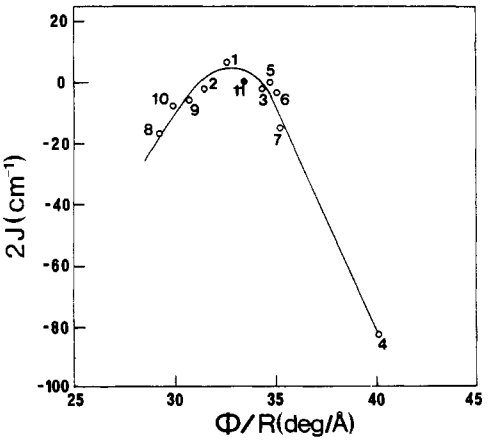

Figure 2. Plot of the singlet–triplet splitting $2J$ vs. ϕ/R for μ-chloro-bridged copper(II) dimers. The data are numbered as in Table I, and the $[Cu(dien)Cl]_2$ dimer position is marked by the black circle. The solid line is a guide for the eye and has no theoretical significance.

tances and angles. A summary of the available data is presented in Table I, and the relationship is plotted in Figure 2. The new ($\Delta E_{ST} = 2J$, ϕ/R) data point is marked by the filled circle in Figure 2, where it may be seen that the magnetic data for $[Cu_2(dien)_2Cl_2](ClO_4)_2$ adhere to the magnetostructural correlation that has been found for all known bis(μ-chloro)-bridged copper(II) complexes.

Shape of EPR Spectrum. The EPR spectrum of a single crystal consists of one or two lines depending on the crystal orientation.

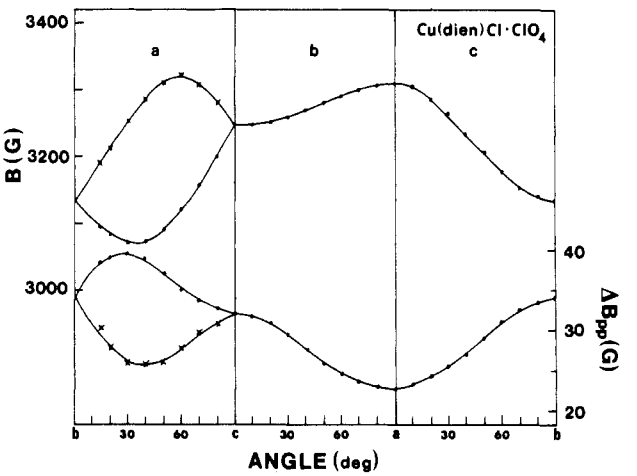

Figure 3. Angular dependence of the resonance field B and line width ΔB_{pp} in the *a*, *b*, *c* crystallographic system. The solid lines on the $B(\theta)$ dependence represent the best fits to eq 4 (see text).

Hyperfine splitting and zero-field splitting (fine structure) were not observed in the spectrum. Hyperfine structure is generally not resolved in EPR spectra of magnetically condensed copper(II) compounds.

The fine structure splitting in exchange-coupled bimetallic copper(II) compounds is expected to have two contributions: (1) an anisotropic exchange contribution as a result of spin–orbit coupling; (2) a contribution from magnetic dipolar coupling between Cu(II) ions. Anisotropic exchange contributions have their maximum values along the z axes of individual copper(II) ions and are given by the expression[12,13]

$$D_z^{ex} = -(g_z - 2)^2 J_1/48 \qquad (2)$$

where the ground state of Cu(II) ion is $d_{x^2-y^2}$ and J_1 is an exchange integral between the ground state $d_{x^2-y^2}$ of one copper(II) ion in a dimer and an excited d_{xy} state of the second ion. This exchange is expected to be ferromagnetic and generally much larger than the exchange ($2J$) that occurs between ground states of the copper(II) ions, as has been proven for a series of bis(μ-hydroxo)-bridged copper(II) complexes[13] and also observed in heterodinuclear complexes.[14]

Even if we can assume J_1 = 2 cm^{-1} in $[Cu_2(dien)_2Cl_2](ClO_4)_2$, i.e. 5 times larger than $2J$, the anisotropic exchange contribution to the total **D** tensor will be on the order of 0.0020 cm^{-1} (about 20 G). Thus, this contribution is negligible compared to that from the intradimer dipolar splitting, which is expected to be largest along the Cu–Cu direction. This dipolar contribution to the **D** tensor can be estimated as D^{dip} (cm^{-1}) = $0.433 g_z^2/r^3$ where r (in

(12) Owen, J.; Harris, E. A. In "Electron Paramagnetic Resonance"; Geshwind, S., Ed.; Plenum Press: New York, 1972; p 427.
(13) Banci, L.; Bencini, A.; Gatteschi, D. *J. Am. Chem. Soc.* **1983**, *105*, 761.
(14) Kahn, O.; Charlot, M. F. *Nouv. J. Chim.* **1980**, *4*, 567.

Å) is the Cu–Cu separation. In $[Cu_2(dien)_2Cl_2](ClO_4)_2$ $r = 3.64$ Å and $D^{dip} = 0.0438$ cm^{-1} (about 450 G). Thus, D^{dip} is about twice as large as that expected for hyperfine splitting from the copper ions. In spite of this quite large D^{dip} value, zero-field splitting is not resolved in the EPR spectrum, although lines from differently oriented complexes are observed in the rotation around the a axis (Figure 3) with splittings even smaller than 450 G. This observation indicates that the zero-field splitting must be dynamically averaged as a result of mobile excitations between magnetically equivalent dimers in the crystal.

For those crystal orientations for which a single EPR line is observed (see rotations b and c in Figure 3), the line shape is Lorentzian and the line width varies from 22 to 34 G at room temperature. In those orientations for which the EPR spectrum contains two lines, the observed line widths are much larger (up to 70 G) and attempts to fit the spectrum with two independent Lorentzian lines were unsuccesful. This result indicates the existence of an exchange interaction between differently oriented dimers in the crystal. The exchange interaction is strong enough to produce the onset of a merging effect of the EPR lines. Evidence for the merging effect is also seen in the sudden narrowing of the EPR lines along the crystallographic axes in the rotation about a where lines from nonequivalent dimers coincide. The latter effect has also been observed in EPR spectra of TCNQ radicals in single crystals where anomalous changes in line width along the crystal axis were related to the jumping rate of excitations between translationally equivalent TNCQ chains.[15]

An EPR spectra with merging lines can be described in terms of stochastic theory[16-18] or in terms of generalized Bloch equations.[19-21] In the secular approximation both theories lead to the same result.[21] The latter approach gives a two-component EPR spectrum shape function $Y(B)$ as a first derivative of out-of-phase magnetization of the system (imaginary part of the total magnetization) in the weak microwave field of the form[21]

$$Y(B) = N\{[W_2 - 2(B - B_0)J]/(W_1^2 + W_2^2) - 4[(B - B_0)W_2 - (\Gamma_0 + 2J)W_1][(B - B_0)W_1 + (\Gamma_0 + J)W_2]/(W_1^2 + W_2^2)^2\} \quad (3)$$

where

$$W_1 = (B - B_a)(B - B_b) - (\Gamma_a + J)(\Gamma_b + J) + J^2$$

$$W_2 = (B - B_a)(\Gamma_b + J) + (B - B_b)(\Gamma_a + J)$$

Γ_j ($j = a, b$) is the half-width of the line and is related to experimentally determined peak-to-peak line width $\Gamma_j = 3^{1/2}\Delta B^j_{pp}/2$. N is a normalization factor and can be related to the total number of paramagnetic centers in the sample or to the total intensity of an experimental spectrum. B_0 and Γ_0 are averaged values of resonance fields and line widths of both lines, respectively. Magnetic fields and line widths are given in gauss in eq 3. The exchange interaction between nonequivalent paramagnetic centers is described by $J(G) = 10697.5J'$ (cm^{-1}) assuming the Hamiltonian $H_{ex} = -J'S_1 \cdot S_2$.

An influence of the merging effect on the EPR spectrum of $[Cu_2(dien)_2Cl_2](ClO_4)_2$ is illustrated in Figure 4, where the experimental spectrum observed along the z axis of a copper(II) complex is presented ($\theta \simeq 30°$ in rotation a). The spectrum was recorded in the magnetic field range 2940–3440 G. The solid line in Figure 4, which is superimposed perfectly on the experimental

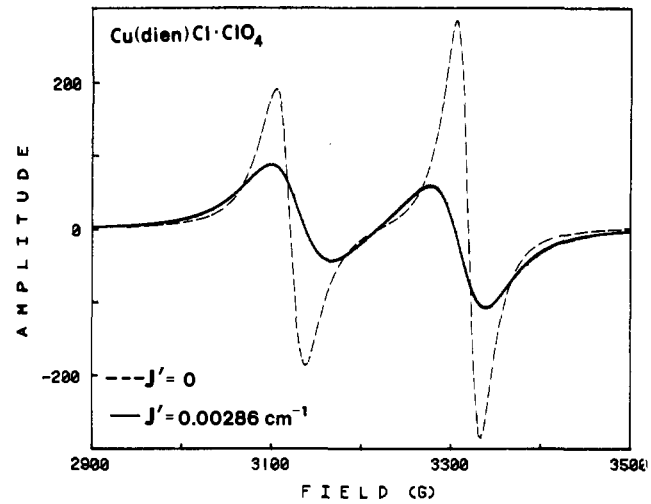

Figure 4. EPR spectrum of $[Cu_2(dien)_2Cl_2](ClO_4)_2$ as observed along the z axis of an individual Cu(II) complex (low-field line) at room temperature. Two theoretical spectra calculated from eq 3 are presented with parameters $B_a = 3120.5$ G, $B_b = 3319.0$ G, $\Delta B^a_{pp} = 33.7$ G, and $\Delta B^b_{pp} = 27.5$ G: (i) solid line (which practically superimposes the experimental spectrum) with $J' = 0.0030$ cm^{-1}; (ii) dashed line with $J' = 0$.

spectrum, represents a theoretical spectrum calculated from eq 3 with $J' = 0.0030$ cm^{-1}. The dashed line represents a theoretical spectrum calculated with the same parameters but with $J' = 0$. It is apparent from Figure 4 that interdimer coupling significantly affects the EPR spectrum. The lines are broadened, and the observed line positions are shifted toward the center of the spectrum by about 30 G. It is clear that true spectral parameters can be found only by calculating theoretical spectra from eq 3 and fitting them to the experimental spectra. All parameters presented in this paper have been found by this method.

Angular Dependence. Angular dependences of the resonance fields and line widths in the orthogonal system a, b, c (Figure 3) indicate that in crystal rotations b and c the lines of nonequivalent dimers are merged completely. An angular g-factor dependence in ith crystal rotation can be described by general $\mathbf{g}^2$ tensor expression[23,24]

$$g^2(i) = \alpha_i + \beta_i \cos 2\theta + \gamma_i \sin 2\theta \quad (4)$$

where θ is the azimuthal angle of the magnetic field. The anisotropy parameters α, β, and γ can be calculated by a least-squares method from a set of equidistant (in angle θ) experimental points from the expression[25]

$$\alpha_i = n^{-1}\sum_{\theta=0}^{M} g^2(\theta)$$

$$\beta_i = 2n^{-1}\sum_{j=0}^{M} g^2(\theta) \cos 2\theta \quad (5)$$

$$\gamma_i = 2n^{-1}\sum_{\theta=0}^{M} g^2(\theta) \sin 2\theta$$

where $n = 36$ and $M = 175°$ for data points collected in 5° intervals and $n = 18$ and $M = 170°$ for 10° intervals. The $B(\theta)$ plots with parameters calculated from eq 5 are presented by solid lines in Figure 3, where a good fit to the experimental points may be seen. A collection of α, β, and γ parameters for three orthogonal rotations enables the determination of the $\mathbf{g}^2$ tensor components. In our case, however, the data in the rotation about a represent individual copper(II) complexes, whereas in rotations about b and c only averaged data are available. By mathematical

(15) Hibma, T.; Kommandeur, J. *Phys. Rev. B: Solid State* **1975**, *12*, 2608.
(16) Yokoda, M.; Koide, S. *J. Phys. Soc. Jpn.* **1954**, *9*, 953.
(17) Abragam, A. "The Theory of Nuclear Magnetism"; Oxford, U.P.: London, 1967; Chapters 4 and 10.
(18) Lenk, R. "Brownian Motion and Spin Relaxation"; Elsevier: Amsterdam, 1977; Chapter 3.
(19) Pople, A.; Schneider, W. G.; Bernstein, H. J. "High-Resolution Nuclear Magnetic Resonance"; McGraw-Hill: New York, 1959; Chapter 10.
(20) Schotland, J.; Leigh, J. S. *J. Magn. Reson.* **1983**, *51*, 48.
(21) Hoffmann, S. K. *Chem. Phys. Lett.* **1983**, *98*, 329.
(22) Atherton, N. M. "Electron Spin Resonance-Theory and Applications"; Halsted Press: New York, 1973; Chapter 7.
(23) Weil, J. A.; Buch, T.; Clapp, J. E. *Adv. Magn. Reson.* **1973**, *6*, 183.
(24) Waller, W. G.; Rogers, M. T. *J. Magn. Reson.* **1975**, *18*, 39.
(25) Hoffmann, S. K.; Corvan, P. J.; Singh, P. Sethulekshmi, C. N.; Metzger, R. M.; Hatfield, W. E. *J. Am. Chem. Soc.* **1983**, *105*, 4608.

Table II. Exchange and EPR Parameters for $[Cu_2(dien)_2Cl_2](ClO_4)_2$

Exchange Integrals (cm^{-1})

$2J = +0.4$ (3) $J' = 0.0030$ (1) (at 295 K)
$J' = 0.0100$ (8) (at 77 K)

EPR Parameters

cryst g factors	direction cosines
$g_3 = 2.166$ (3)	(0, 1, 0)
$g_2 = 2.093$ (3)	(0, 0, 1)
$g_1 = 2.054$ (3)	(1, 0, 0)
molec g factors	**direction cosines**
$g_z = 2.214$ (3)	(−0.0204, 0.8481, −0.5294)
$g_y = 2.057$ (3)	(−0.9847, −0.0751, −0.1581)
$g_x = 2.046$ (3)	(−0.1738, 0.5244, 0.8335)

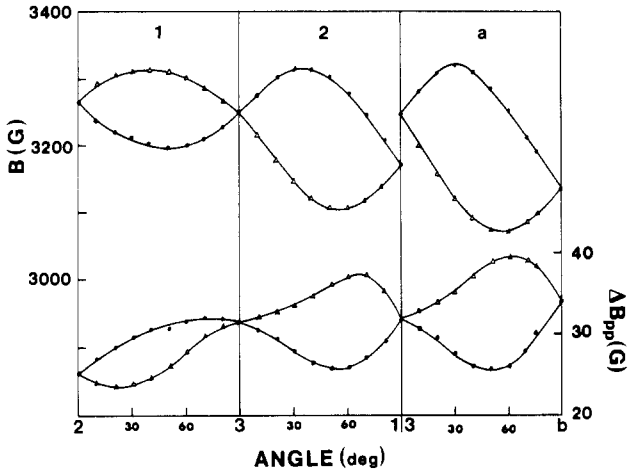

Figure 5. Angular dependence of the resonance fields and line widths in the *1*, *2*, *a* coplanar reference system, where two resonance lines are observed. Solid lines in $B(\theta)$ plots represent the best fit to eq 3.

averaging of two line positions in the rotation about *a* and fitting the results with eq 4, the averaged anisotropy parameters were obtained and the crystal tensor components were calculated as

$$\mathbf{g}_{cr}^2 = \begin{bmatrix} \alpha_c+\beta_c & \gamma_c & \gamma_b \\ \gamma_c & \alpha_a+\beta_a & \gamma_a \\ \gamma_b & \gamma_a & \alpha_b+\beta_b \end{bmatrix} \quad (6)$$

Standard matrix diagonalization leads to the principal values and direction cosines that are summarized in Table II. The *G* factors ($g_3 = 2.166$, $g_2 = 2.093$, $g_1 = 2.054$) obtained by this method represent averaged crystal values.

Molecular *g* factors of the individual Cu(II) complexes can be found by using a general mathematical decoupling procedure[26] and crystal *g* factors and angles of the complex orientation calculated from crystal data. We have used, however, a direct method for the determination of molecular *g* factors from the experimental data. Angular dependences of the spectra were measured in two additional crystal rotations around axes *1* and *2*. The axes *1* and *2* are mutually perpendicular and lie in the crystal *ab* plane with an angle $\theta = 60°$ between axes *1* and *a* and an angle of 30° between *a* and *2*. In both rotations two EPR lines are resolved. Resonance fields and peak-to-peak line widths ΔB_{pp}, obtained by computer simulation with eq 3, are presented in Figure 5 together with data from rotation about *a*. The axes *1*, *2*, *a* form a coplanar system and anisotropy parameters α, β, and γ in rotations *1*, *2*, and *a* can be used to form the $\mathbf{g}^2$ tensor in the *a*, *b*, *c* orthogonal system by using the general Waller–Rogers method.[27] This

(26) Hoffmann, S. K.; Szczepaniak, L. S. *J. Magn. Reson.* **1983**, *52*, 182.
(27) Waller, W. G.; Rogers, M. T. *J. Magn. Reson.* **1973**, *9*, 92.

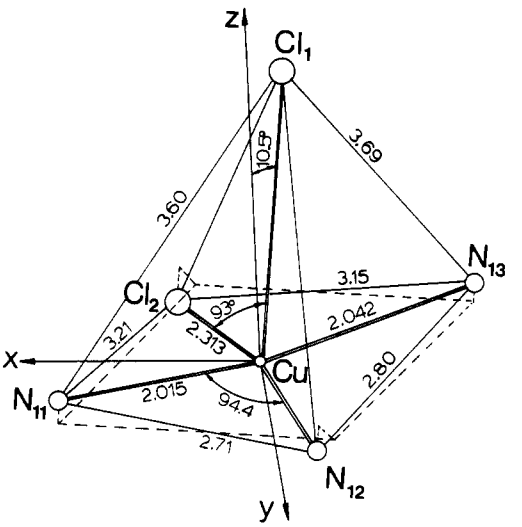

Figure 6. Geometry of the coordination sphere of copper in $[Cu_2(dien)_2Cl_2]^{2+}$. The axes *x*, *y*, and *z* are the principal axes of the EPR **g** tensor.

Table III. Molecular **g** Tensor Axes Orientation (deg) with Respect to the Coordination Sphere of an Individual Copper(II) Ion in $[Cu_2(dien)_2Cl_2](ClO_4)_2$

	z	*y*	*x*
apical Cu-Cl1	10.5	80.5	85.7
basal Cu-Cl2	77.9	54.8	142.2
trans N11-N13	96.1	39.3	38.6

method used with our experimental axes setting gives a molecular $\mathbf{g}^2$ tensor in the form

$$\mathbf{g}_{mol}^2 = \begin{bmatrix} W_{aa} & W_{ab} & W_{ac} \\ W_{ab} & \alpha_a+\beta_a & \gamma_a \\ W_{ac} & \gamma_a & \alpha_a-\beta_a \end{bmatrix} \quad (7)$$

where

$$W_{aa} = \alpha_a = \beta_a + 2(\beta_2 - \beta_1)/(\cos 2\psi)$$

$$W_{ab} = 2\beta_a/(\sin 2\psi) + 2(\beta_2 \sin^2\psi - \beta_1 \cos^2\psi)/(\sin 2\psi \cos 2\psi) \quad (8)$$

$$W_{ac} = (\gamma_a \sin\psi - \gamma_2)/(\cos\psi)$$

In all three rotations in the coplanar system there are two $B(\theta)$ plots (Figure 5) that have identical α, β, and γ coefficients but differ in the sign of the γ value. Thus, as can be seen from eq 8, it is generally possible to form eight different tensors (eq 7) with different signs of γ_a and different signs and values of W_{ac}. Diagonalization of these tensors indicated that there are two different sets of eigenvalues and eigenvectors but only one of these contains acceptable molecular *g* factors, those being $g_z = 2.214$, $g_y = 2.057$, and $g_x = 2.046$. Direction cosines of molecular *x*, *y*, *z* axes are summarized in Table II, and the molecular axes directions are shown in Figure 6. The angles between the *x*, *y*, and *z* axes and molecular directions in the $[Cu(dien)Cl_2]$ complex are given in Table III. Because of low complex symmetry the *g*-factor axes are not determined by copper–ligand directions. The *z* axis deviates by about 10° from the $Cu-Cl_{apical}$ direction toward the basal Cl, and the *y* and *x* axes deviate significantly from trans-basal directions N–Cl and N–N, respectively.

There are four dimeric units in the unit cell of $[Cu_2(dien)_2Cl_2](ClO_4)_2$.[7] Thus, there are four pairs of differently oriented Cu(II) complexes, and the *z* axes of these form angles of 29° with the crystallographic *c* axis. In crystal rotations *1* and *2*, the two EPR lines correspond to different pairs of copper(II) complexes, and computer fitting to eq 3 permits the determination of the interdimer exchange value *J'*. *J'* can differ between different pairs of complexes. The results of the fitting indicate, however, that the exchange interaction is the same between all magnetically

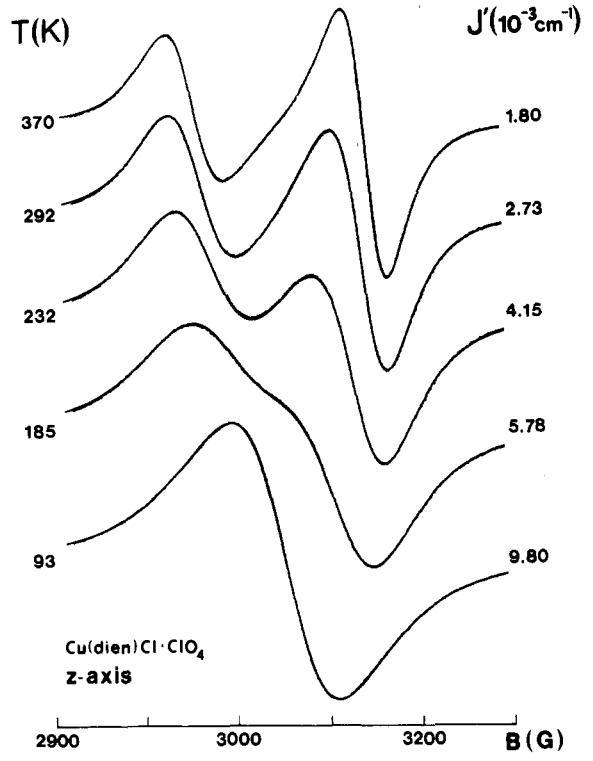

Figure 7. Temperature dependence of the EPR spectrum observed along the molecular z axis in $[Cu_2(dien)_2Cl_2](ClO_4)_2$. The lines broaden, and the interdimer exchange J' increases with decreasing temperature.

nonequivalent dimers, with $J' = 0.0030$ (1) cm^{-1} at room temperature.

Temperature Dependence of the EPR Spectrum. The EPR spectra of $[Cu_2(dien)_2Cl_2](ClO_4)_2$ display unusual temperature dependences. The resonance lines broaden with decreasing temperature in all crystal orientations. This behavior is opposite to that normally observed in paramagnetic crystals. The temperature dependence was recorded along crystallographic axes, where a single line is observed, and along the molecular z axis where two lines exist in the spectrum. The temperature dependence of the EPR spectrum along the z axis is presented in Figure 7 together with spectra calculated from eq 3 and the resulting J' integrals. Two effects can be seen in Figure 7: the lines become broader and the interdimer exchange J' increases with decreasing temperature. As a result, the lines merge completely at about 90 K. Figure 8 demonstrates that the line width–temperature behavior is similar in all measured crystal orientations. It can be seen from this figure that at least two different competing mechanisms determine the ΔB_{pp} temperature dependence. In the high-temperature region (above room temperature), ΔB_{pp} varies weakly with temperature, and in spectra along the b- and c-axis directions the line width displays a small increase with temperature. In the low-temperature region (below 250 K), a second mechanism dominates the line width and ΔB_{pp} increases linearly with decreasing temperature down to 77 K. This is unusual behavior.

The dipolar line width resulting from an interdimer magnetic interaction is expected to have its maximum value close to the z-axis direction with $\Delta B_{pp} \sim 50$ G, since the interdimer distance is shortest ($\sim$7.5 Å) in this direction. The suggestion that the room-temperature line width is determined mainly by interdimer dipolar coupling is confirmed by angular line width dependences (Figures 3 and 5) that display maxima close to those in $B(\theta)$ dependence as is expected for the anisotropic dipolar interaction. In such cases, it is reasonable to expect no temperature dependence of the EPR line width as has been observed in some three-dimensional magnetic systems with weak exchange interactions.[28,29]

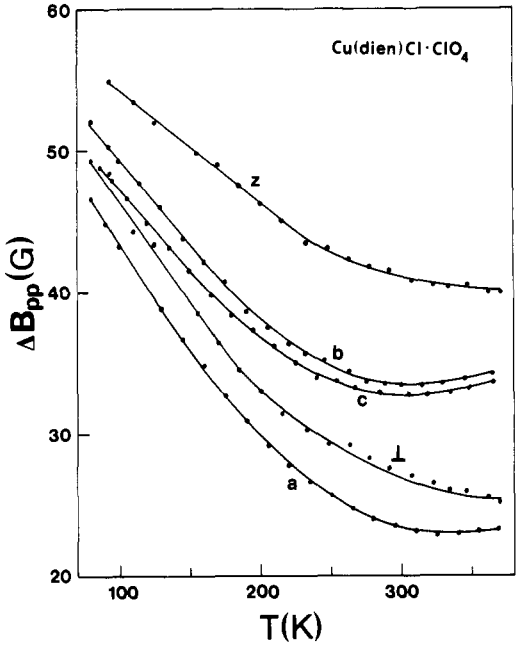

Figure 8. Temperature variations of the line widths as observed along the crystallographical axes a, b, and c, along the molecular z axis, and in a direction perpendicular to the z axis.

Standard theories of the line width also predict no temperature dependence.[30-32] In most crystals, however, ΔB_{pp} varies with temperature. This behavior is explained in various ways including a variation in spin–lattice relaxation via phonon modulation of the electric crystal field,[33] phonon modulation of antisymmetric exchange,[34-36] anharmonic crystal lattice effects in exchange coupling,[31,32,37] and lifetime effects.[32,38] All the above mechanisms lead to a "normal" decrease of ΔB_{pp} with temperature.

Broadening of the EPR lines at low temperatures can be explained in terms of precritical fluctuations in the system close to the critical temperature T_C or T_N[39-41] or in terms of the temperature dependence of the triplet state population since dipolar coupling is proportional to the probability that the dimers are in the triplet state.[38] In $[Cu_2(dien)_2Cl_2](ClO_4)_2$ both J and J' are too small for these effects to contribute to the temperature dependence of the linewidth.

The temperature dependence of ΔB_{pp} in $[Cu_2(dien)_2Cl_2](ClO_4)_2$ can be explained as arising from unresolved zero-field splitting, which is expected from intradimer dipolar coupling. This coupling is expected to lead to the splitting of the observed EPR lines into doublets with splitting of about 450 G as was noted above. This fine structure is not resolved at high temperatures but does determine the line width value. The mobility of the excitation and dynamical averaging of the fine structure decrease with decreasing temperature. At very low temperature, where the triplet excitation is expected to be immobile, a resolution of the fine structure should occur. This effect has been observed in $[Co(en)_3]_2[Cu_2Cl_8]$-$Cl_2 \cdot 2H_2O$.[42]

(28) Okuda, K.; Hata, H.; Date, M. *J. Phys. Soc. Jpn.* **1972**, *33*, 1574.
(29) Soos, Z. G.; Huang, T. Z.; Valentine, J. S.; Hughes, R. C. *Phys. Rev. B: Solid State* **1973**, *8*, 993.
(30) Richards, P. M.; Salamon, M. B. *Phys. Rev. B: Solid State* **1974**, *9*, 32.
(31) Soos, Z. G.; McGregor, K. T.; Cheung, T. T. P.; Silverstein, R. J. *Phys. Rev. B: Solid State* **1977**, *16*, 3036.
(32) Cheung, T. T. P.; Soos, Z. G. *J. Chem. Phys.* **1978**, *69*, 3845.
(33) Drumheller, J. E.; Zaspel, C. E. *Physica B+C (Amsterdam)* **1977**, *86*, 1025.
(34) Seehra, M. S.; Castner, T. G. *Phys. Kondens. Mater.* **1967**, *7*, 185.
(35) Castner, T. G.; Seehra, M. S. *Phys. Rev. B: Solid State* **1971**, *4*, 38.
(36) Willett, R. D.; Wong, R. J. *J. Magn. Reson.* **1981**, *42*, 446.
(37) Zaspel, C. E.; Drumheller, J. E. *Phys. Rev. B: Solid State* **1977**, *18*, 1771.
(38) McGregor, K. T.; Soos, Z. G. *Inorg. Chem.* **1976**, *15*, 2159.
(39) Battles, J. W. *J. Appl. Phys.* **1971**, *42*, 1286.
(40) Seehra, M. S. *J. Appl. Phys.* **1971**, *42*, 1290.
(41) Tazuke, Y.; Nagata, K. *J. Phys. Soc. Jpn.* **1975**, *38*, 1003.
(42) McGregor, K. T.; Hatfield, W. E. *J. Chem. Phys.* **1976**, *65*, 4155.

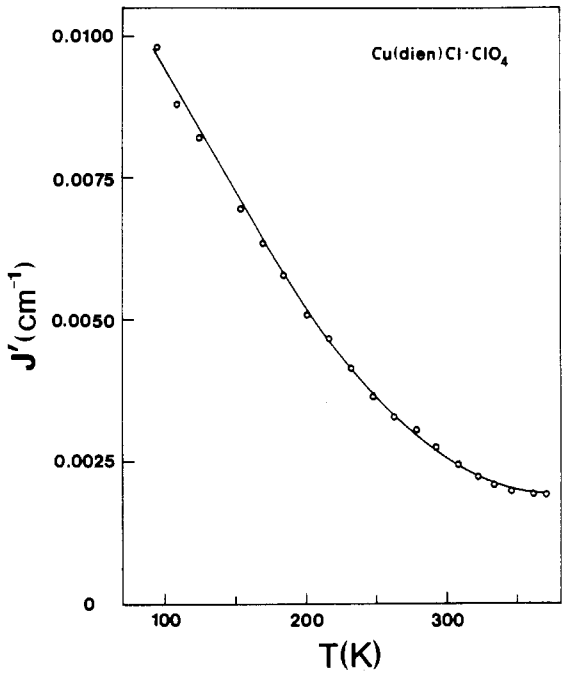

Figure 9. Temperature dependence of the interdimer exchange integral J' in $[Cu_2(dien)_2Cl_2](ClO_4)_2$.

Temperature Dependence of Exchange Coupling. The interdimer exchange integral J' exhibits similar behavior to ΔB_{pp}; i.e., it increases with decreasing temperature (Figure 9), even though these two effects are mutually independent. A temperature dependence of the exchange interaction has been documented in a few instances. In $K_2CuCl_4 \cdot 2H_2O$, a merging effect of EPR lines has been observed[43,44] and an increase in the exchange integral from $J = 0.09$ cm^{-1} at 300 K to $J = 0.17$ cm^{-1} at 77 K has been found. The behavior was explained in terms of a temperature dependence of the intercopper distances by taking the thermal average of J over the vibrational states of an anharmonic oscillator.[37] An increase in the intradimer coupling with decreasing temperature has been found in the copper(II) dimers $[Cu_2(tren)_2(OCN)_2](BPh_4)_2$ and $[Cu_2(tren)_2(SCN)_2](BPh_4)_2$ from direct observation of singlet–triplet transitions in the EPR spectra.[45] A small increase in the intradimer J value at low temperature has been measured directly from optical and luminescence spectra of exchange-coupled chromium(III) dimers ($J = 24$ cm^{-1}) in $[Cr_2(OH)_2en_4]I_4$,[46] and neutron inelastic scattering data in $[Cr_2(OH)(NH_3)_{10}]Cl_5 \cdot H_2O$[47] has been interpreted in terms of a temperature dependence of the exchange interaction. A temperature-dependent J value is often postulated when it is not possible to fit bulk magnetic susceptibility data over wide temperature ranges to theoretical models, e.g., in $(C_3H_7NH_3)_2MnCl_4$ and $(C_3H_7NH_3)MnBr_4$[48] and in $Cu(n\text{-}C_3H_7nso)NO_3$.[49]

In all of the cases cited above, the exchange integral increases at low temperatures in a manner similar to that observed in $[Cu_2(dien)_2Cl_2](ClO_4)_2$ and this behavior can be explained in terms of a decrease in interionic distances as a result of thermal lattice contraction. This effect is expected to be larger for interdimer exchange than for intradimer exchange; thus, the relative increase in J' is much larger than that found for J values.

A merging effect with decreasing temperatures is found in the EPR of $(C_7H_7)^+[Ni(mnt)_2]^-$ with a corresponding increase of J' (interstack exchange) from 0.015 cm^{-1} at room temperatures to 0.053 cm^{-1} at 4.2 K. The crystal parameters were measured at various temperatures and were found to decrease with decreasing temperatures.[50]

A theoretical description of $J(T)$ dependence must take into account other mechanisms that can affect this temperature dependence. Superexchange interactions are expected to be proportional to overlap integrals between atomic orbitals in superexchange pathways. Orbital overlapping is modulated by thermal lattice vibrations and depends on the average amplitude of the atomic displacements that are temperature dependent. Thus interdimer J' values can increase with temperature as a result of increased overlap with increasing vibrational amplitudes. This behavior has been observed in $[Co(en)_3]_2[Cu_2Cl_8]Cl_2 \cdot 2H_2O$[21] and in $[N(n\text{-}Bu)_4]_2[Cu(mnt)_2]$.[51] A temperature dependence of the exchange integral can also be caused by an exchange elasticity effect as has been observed in dinuclear copper(II) cryptates[52] where the J value decreases strongly at low temperatures.

Acknowledgment. This research was supported by the National Science Foundation (Grant No. CHE 83 08129).

Registry No. $[Cu(dien)Cl]_2(ClO_4)_2$, 90186-95-1.

(43) Kennedy, T. A.; Sung Ho Choh; Seidel, G. *Phys. Rev. B: Solid State* **1971**, *2*, 3645.
(44) Okuda, T.; Date, M. *J. Phys. Soc. Jpn.* **1970**, *28*, 308.
(45) Duggan, D. M.; Hendrickson, D. N. *Inorg. Chem.* **1974**, *13*, 2929.
(46) Beutler, A.; Güdel, H. U.; Snellgrove, T. K.; Chapuis, G.; Schenk, K. *J. Chem. Soc., Dalton Trans.* **1979**, 983.
(47) Güdel, H. U.; Furrer, A. *Mol. Phys.* **1977**, *33*, 1335.
(48) Groenendijk, H. A.; Duyneveldt, A. J.; Willett, R. D. *Physica B+C (Amsterdam)* **1979**, *98*, 53.
(49) (a) Mikuriya, M.; Okawa, H.; Kida, S. *Bull. Chem. Soc. Jpn.* **1982**, *54*, 2979. (b) Nakatsuka, S.; Osaki, K.; Uryu, N. *Inorg. Chem.* **1982**, *21*, 4332.
(50) Manoharan, P. T.; Noordik, J. H.; de Boer, E.; Keijzers, C. P. *J. Chem. Phys.* **1981**, *74*, 1980.
(51) Plumlee, K. W.; Hoffman, B. M.; Ibers, J. A.; Soos, Z. G. *J. Chem. Phys.* **1975**, *63*, 1926.
(52) Kahn, O.; Morgenstern-Badarau, I.; Audiere, J. P.; Lehn, J. M.; Sullivan, S. A. *J. Am. Chem. Soc.* **1980**, *102*, 5935.
(53) Svedung, D. H. *Acta Chem. Scand.* **1969**, *23*, 2865.
(54) Watkins, N. T.; Dixon, E. E.; Crawford, V. H.; McGregor, K. T.; Hatfield, W. E. *J. Chem. Soc., Chem. Commun.* **1973**, 133.
(55) Megnamisi-Belombe, M.; Novotny, M. A. *Inorg. Chem.* **1980**, *19*, 2470.
(56) Phelps, D. W.; Goodman, W. H.; Hodgson, D. J. *Inorg. Chem.* **1976**, *15*, 2266.
(57) Estes, W. E. Ph.D. Dissertation, The University of North Carolina at Chapel Hill, 1977.
(58) Carrabine, J. A.; Sundaralingam, M. *J. Am. Chem. Soc.* **1970**, *92*, 369. DeClerq, J. P.; Debboudt, M.; vanMeersche, M. *Bull. Soc. Chim. Belg.* **1971**, *80*, 527. Sundaralingam, M.; Carrabine, J. A. *J. Mol. Biol.* **1971**, *61*, 287.
(59) Drake, R. F.; Crawford, V. H.; Laney, N. W.; Hatfield, W. E. *Inorg. Chem.* **1974**, *13*, 1246. Villa, J. F. *Inorg. Chem.* **1973**, *12*, 2054.
(60) Hodgson, D. J.; Hale, P. K.; Hatfield, W. E. *Inorg. Chem.* **1971**, *10*, 1061.
(61) Barnes, J. A.; Hatfield, W. E.; Hodgson, D. J. *Chem. Phys. Lett.* **1970**, *7*, 374. McGregor, K. T.; Losee, D. B.; Hodgson, D. J.; Hatfield, W. E. *inorg. Chem.* **1974**, *13*, 756.
(62) Swank, D. D.; Needham, G. F.; Willett, R. D. *Inorg. Chem.* **1979**, *18*, 761.
(63) Estes, E. D.; Estes, W. E.; Hatfield, W. E.; Hodgson, D. J. *Inorg. Chem.* **1975**, *14*, 106.
(64) Marsh, W. E.; Hatfield, W. E.; Hodgson, D. J. *Inorg. Chem.* **1982**, *21*, 2679.
(65) Duckworth, V. F.; Stephenson, N. C. *Acta Crystallogr., Sect. B: Struct. Crystallogr. Cryst. Chem.* **1969**, *B25*, 1975.
(66) Jeter, D. Y.; Hodgson, D. J.; Hatfield, W. E. *Inorg. Chim. Acta* **1971**, *5*, 257.